Plasmonic Infrared Attenuator

Pedro N Figueiredo
Truventic, LLC
Orlando, USA
p.figueiredo@truventic.com

Robert E Peale
Truventic, LLC
Orlando, USA
peale.truventicllc@gmail.com

***Abstract*— A variable attenuator for high-powered IR beams, based on MEMS-controlled excitation of surface plasmon polaritons on suitably conducting surfaces is described. Materials choice determines the useful spectral band. Intensity variation over nine-orders is theoretically possible.**

Keywords*— *Surface Plasmon Polariton, Plasmonic Attenutation, Attenuator, Otto Configuration, Epsilon Near Zero

I. Introduction

Fast amplitude modulation of infrared laser intensity has applications to telemetry, laser machining, and infrared scene simulators. A number of external variable attenuators are known, including partially-absorbing materials of variable thickness [1], diffractive metal screens [2], wire grid attenuators [3], pinhole attenuator [4], variable-angle etalons [5], and rotating ZnSe Brewster- angle "pile of plates" polarizers [6]. None of these allow rapid variations of attenuation, and the range of attenuation is typically less than three orders of magnitude.

Here we present a design for a variable attenuator of polarized infrared laser beams based on absorption by a conducting surface due to excitation of surface plasmon polaritons (SPP). In principle, this attenuator could handle high laser powers because the absorption occurs on the surface of a solid whose thermal properties and heat-sinking can be engineered. Variable extinction ratios of up to 9 orders of magnitude are predicted via a mechanical displacement of only a few microns. Such displacement could be realized using suitable piezo-electric actuators, so that changes could be sufficiently fast for useful amplitude modulation.

II. Background

The innovation is based on the well-known "Otto-coupler" [7], which is depicted schematically in Figure 1. Strong transverse-magnetic (TM) polarized light, indicated by the thick arrows and incident at the SPP excitation resonance angle, which lies beyond the critical angle for total internal reflection Θ_{TIR}, excites SPPs on a conducting surface. These lossy bound electromagnetic waves propagate to the right as indicated and decay into heat. Their fields are exponentially damped away from the surface, as suggested in Figure 1. The close-coupled prism is essential to the light-to-SPP conversion. The attenuated reflected intensity, indicated by the thin arrows, depends strongly on the gap dimension d.

This work was supported by an U. S. Air Force STTR Phase I award, Topic AF17A-T022, Joshua Lentz Program Manager, Eglin AFB

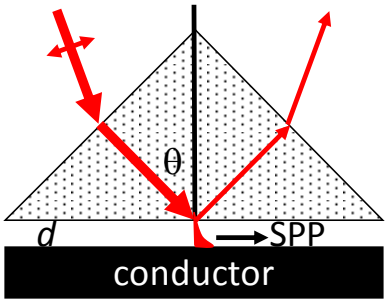

Figure 1. Schematic of Otto coupler for excitation of surface plasmon

To support an SPP, the plasma wavelength of the conductor must be shorter than the infrared operating wavelength. Though easily satisfied for all usual metals, such metals present significant practical disadvantages. We will demonstrate that the conductor should be chosen so that its plasma wavelength is only a little shorter than the operating wavelength.

SPP momentum is less than that of free-space photons of the same frequency. The Otto-coupler prism slows the incident photon so that its momentum can match that of the SPP. The momentum matching condition gives an excitation-resonance incidence-angle Θ_{SPP}, according to [7, 8]

$$\sin\Theta_{SPP} = (1/n)\ \mathrm{Re}(\sqrt{(\varepsilon/(\varepsilon+1))}) \qquad (1)$$

where n is the prism's real refractive index and $\varepsilon = \varepsilon' + i\varepsilon''$ is the frequency-dependent complex permittivity of the conductor. Equation (1) resembles the condition for total internal reflection (TIR) of the prism, namely

$$\sin\Theta_{TIR} = 1/n \qquad (2)$$

To support an SPP [8], the conductor should have $\varepsilon' < 0$ and $|\varepsilon'| >> \varepsilon'' > 0$. Hence, the SPP excitation resonance is always observed at incidence angles Θ_{SPP} that exceed the critical angle Θ_{TIR}. However, if $|\varepsilon'| >> 1$, the angles Θ_{SPP} and Θ_{TIR} are almost equal, which would complicate control of the proposed attenuator. To obtain a Θ_{SPP} that significantly exceeds Θ_{TIR} requires a small (negative) value for ε', which occurs when the plasma wavelength λ_p is only a little shorter than the operating wavelength λ. For purposes of this work, the plasma wavelength can be identified as that where the real part of the permittivity passes through zero and changes sign.

The SPP fields decay exponentially away from the surface with a characteristic length L (the SPP mode height) given by [8]

$$1/L = (2\pi/\lambda)\ \mathrm{Re}(\sqrt{[-1/(\varepsilon+1)]}) \qquad (3)$$

978-1-7281-0602-1/19/$31.00 ©2019 IEEE

The SPP resonance condition Eq. (1) tells nothing about the resonance strength or angular line shape. However, these are accurately calculated using the well-known analytic Fresnel equations for a three-layer system (prism/air/conductor) [9]. In this work, experiments and calculations were first performed at visible wavelengths to confirm agreement. Then we performed design calculations in the infrared for different conductors. Finally, we performed infrared experiments using an optimized conductor for those wavelengths and compare the results with theory.

III. Experimental Details

SPP resonance experiments were performed at visible wavelengths using a BK7 prism and a gold-coated microscope slide. Imperfections and dust on the surfaces give air gap of a few microns when the prism and slide are mated. The air gap was adjusted between 0.3 and 0.6 µm using pressure from a screw on the back of the microscope slide. The transverse magnetic (TM) polarized beam from a laser diode with 650 nm wavelength was incident, as shown in Figure 1, with the electric field in the plane of the figure. Specular reflectance was measured using a Θ-2Θ motorized goniometer [10] and a silicon detector.

Experiments at 5.6 µm wavelength were performed using a TM polarized quantum cascade laser [11], a CaF_2 prism (Thorlabs) and a thermopile detector (Coherent Powermax USB). The conductors for these experiments were differently fluorine-doped films of tin-oxide (F:SnO_2, or "FTO", SISOM Thin Films) grown on glass. Thorough characterization of these samples relevant to SPPs was reported in [12-14].

IV. Material Considerations

We [15-20] and others [21] have investigated a number of materials having infrared plasma wavelengths. Figure 2 presents SPP resonance angles (solid red square symbols) calculated from Equation (1) at an operating wavelength of 5.6 µm for several representative materials spanning a range of plasma wavelengths. The horizontal dashed red line labeled (TIR) in Figure 2 gives the critical angle. All of the resonances angles are beyond the critical angle, as already mentioned. The resonances angles increase as the plasma wavelength increases toward the operating wavelength.

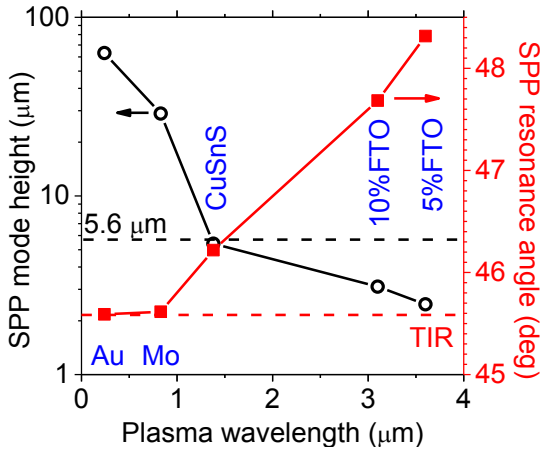

Figure 2. SPP resonance angle and mode height vs. plasma wavelength for different conductors at 5.6 µm operating wavelength

Figure 2 also presents the SPP mode height L as a function of plasma wavelength for the same set of materials. A horizontal dashed line indicates the mode height that equals the 5.6 µm operating wavelength. The SPP tends to become more confined as the plasma wavelength of the conductor increases toward the operating wavelength. For gold the L value is 12 times larger than the operating wavelength. For the 5% FTO sample, L is twice smaller than this wavelength. Our calculations (below) show that the SPP mode height gives roughly the gap value required for optimal Otto-coupling and maximum attenuation.

We next present experimental results at visible wavelengths to demonstrate the strong dependence of attenuation on gap and the accuracy of the Fresnel calculations.

V. Experimental Results

Figure 3 presents measured and calculated angular reflectance spectra for an Otto coupler comprising BK7 prism, air gap, and Au film. The experimental reflected intensity curves were normalized to their values at 50°, where there is little or no attenuation. As predicted by calculations presented in Figure 2, the experimental resonance angles are beyond the critical angle indicated by the vertical dashed line. The experimental gap dimensions were determined by varying d in the calculation utilizing a Chi-squared goodness-of-fit minimization. The best fit calculations (black lines) closely match experimental curves. A change in gap by 0.225 µm changes the attenuation from ~48% to ~99% at an incidence angle of ~42.6 deg.

Figure 4 (right) presents Fresnel-calculated reflectance vs. incidence angle for the same five conductors considered in Figure 2. One sees that for metals with $\lambda_p << \lambda$, the resonance occurs close to the indicated TIR angle and such resonances are inconveniently sharp. On the other hand as λ_p approaches λ, the resonances become increasingly broad, which is convenient for optical alignment. Apparently, the minimum transmittance is independent of plasma wavelength. In other words, any conductor with $\lambda_p < \lambda$ can provide a "100 %" deep resonance at the optimum gap *d*, but those with longer plasma wavelength would be more practical.

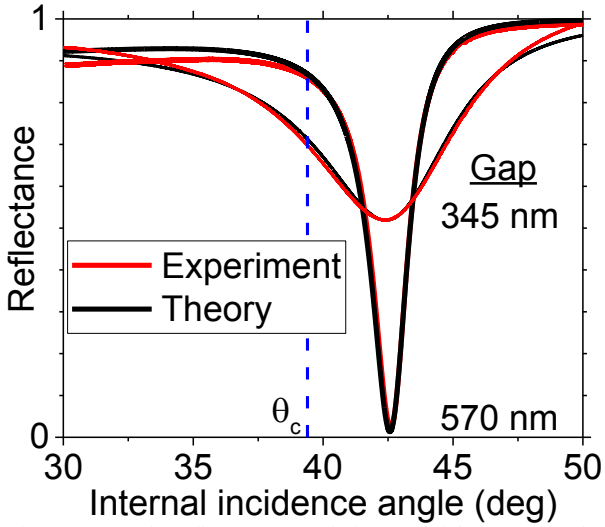

Figure 3. Specular reflectance vs angle for BK7/Air/Au Otto-coupler at 650 nm wavelength.

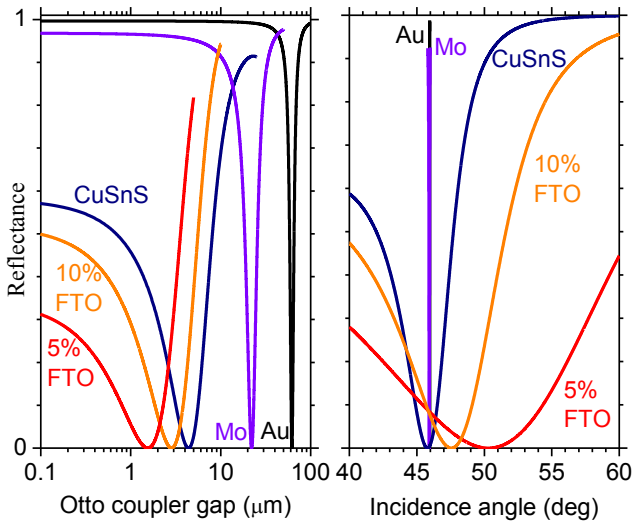

Figure 4. CaF_2-based Otto coupler reflectance at 5.6 μm operating wavelength as a function of gap at optimum angle (left) and as function of angle at optimum gap (right) for different conductors.

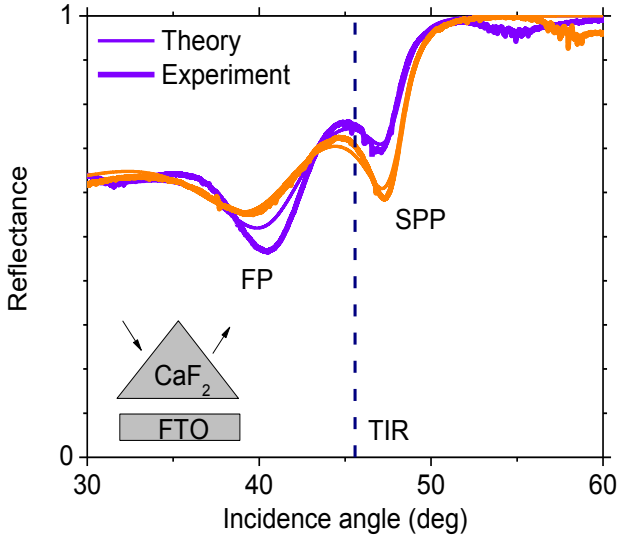

Figure 5. Measured and Fresnel-calculated angular reflectance spectra for an Otto coupler comprising CaF2 prism, air gap, and FTO at 5.6 μm operating wavelength for two different air gaps.

Figure 4 (left) presents reflectance for the considered materials as a function of air gap at the optimum angle of incidence for 5.6 μm operating wavelength. The horizontal axis is logarithmic in this case. When $\lambda_p << \lambda$, as for gold, resonances occur at gaps that exceed 10 μm and they change with gap over ~10 μm scales. When λ_p approaches λ, as for FTO, resonances occur at $d \sim 1$ μm and they change significantly for gap changes of only a few microns, which would be much more convenient for control by a piezoelectric actuator. The calculations predict changes in reflectance with gap by 9 orders of magnitude. We consider the practicality of experimentally achieving this below.

By comparing Figure 4 (left) with Figure 2, we see that coupling is always optimized for maximum attenuation when d ~ L. For instance, the minimum reflectance for 10% FTO occurs at a gap of 3 μm in Figure 4 (left), and the SPP mode height for this material from Figure 2 is also 3 μm.

Figure 5 presents measured and Fresnel-calculated angular reflectance spectra for an Otto coupler comprising CaF_2 prism, air gap, and FTO at 5.6 μm operating wavelength for two different air gaps. The air gap values were found in the same way as for Figure 3. Below TIR we find a dip that can be attributed to a Fabry-Perot type resonance. Attenuation for this feature is caused probably by the beam being wave-guided within the gap via multiple reflections at resonance, resulting in a lateral translation, so that collection efficiency at the detector is reduced. Above TIR, we find the expected SPP resonance. Agreement between experiment and calculation is very good for the SPP resonance.

Figure 6 presents a calculation of reflectivity vs. gap at the angle of maximum attenuation for a CaF_2/air/FTO Otto coupler. The two curves are the same data plotted linearly and semi-logarithmically. The linear plot shows that a tenfold change in attenuation can be achieved with a gap change of ~1.5 microns. The semi-log plot shows that an attenuation by 9 orders of magnitude can be achieved in principle. However, expectations should be modified due to practical considerations. At the highest attenuation, the curve is very step, so that positional control of ~10 nm would be required. It might be difficult to arrange an FTO sample that is even that smooth, considering that grain-sizes of this typically polycrystalline material are at least that large [12]. However, attenuation by up to 10000 times might be practical and controllable, which is better than usually obtained in laboratory and commercial attenuators [1-6]. The plasmonic device presented here has the advantage that the attenuation might be rapidly changed under electronic control.

VI. Discussion and Summary

A laser attenuator based on infrared intensity loss to surface plasmon polariton generation has been proposed. Design calculations are verified by initial experiments. Practical considerations indicate that the conductor that serves as SPP host should have plasma wavelength just a little below the operating wavelength.

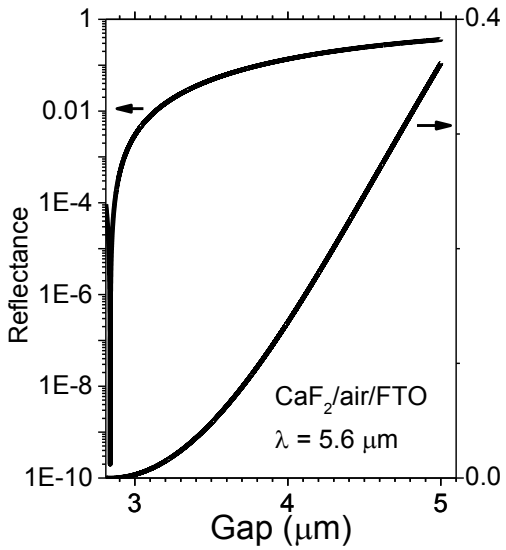

Figure 6. Calculated reflectance vs. gap at optimum angle for CaF2/air/FTO Otto-coupler at 5.6 μm operating wavelength.

VII. Acknowledgments

We thank Prof. Arkadiy Lyakh, University of Central Florida for loan of the QCL and Thermopile detector and Prof. A. J. Sievers, Cornell University for the donation of the motorized goniometer.

References

[1] R. E. Peale, K. Muro, J. T. McWhirter and A. J. Sievers, "Incoherent saturation study of the selenium donor in AlSb," Sol. State Comm. 60, 753 (1986).

[2] Fritz Keilmann, "Precision Broadband Far-Infrared Attenuator," Proc. SPIE 666, 213 (1986).

[3] S. D. Hanton, "Variable attenuator for high‐power lasers." Rev. Sci. Inst. 64, 1456 (1993).

[4] S. E. Bialkowski, "Simple scheme for variable high‐power laser beam attenuation," Rev. Sci. Inst. 58, 2338 (1987).

[5] Wavelength Tech, BLK 2, Bukit Batok St.24, #06-03, Skytech Building, Singapore 659480.

[6] II-VI Infrared, 375 Saxonburg Blvd , Saxonburg, PA 16056, United States

[7] A. Otto, "Excitation of nonradiative surface plasma waves in silver by the method of frustrated total reflection," Z. Phys. 216, 398 (1968).

[8] L. D. Landau, E. M. Lifshitz, and L. P. Pitaevskii, Electrodynamics of Continuous Media, 2nd ed. (Butterworth-Heinemann, Oxford, 1984) Section 88, problem.

[9] L. D. Landau, E. M. Lifshitz, and L. P. Pitaevskii, Electrodynamics of Continuous Media, 2nd ed. (Butterworth-Heinemann, Oxford, 1984) Section 86, problem 4.

[10] Z. Schlesinger, B. C. Webb, A. J. Sievers, "Attenuation and coupling of far infrared surface plasmons," Solid State Communications 39, 1035 (1981).

[11] P. Figueiredo, M. Suttinger, R. Go, A. Todi, Hong Shu, E. Tsvid, C. Kumar, N. Patel, A. Lyakh, "High performance 40-stage and 15-stage quantum cascade lasers based on two-material active region composition," Proc. SPIE 10194, 101942L (2017).

[12] F. Khalilzadeh-Rezaie, I. O. Oladeji, J. W. Cleary, N. Nader, J. Nath, I. Rezadad, and R. E. Peale, "Fluorine-doped tin oxides for mid-infrared plasmonics," Optical Materials Express 5, 2184-2192 (2015).

[13] R. E. Peale, E. Smith, H. Abouelkhair, I. O. Oladeji, S. Vangala, T. Cooper, G. Grzybowski, F. Khalilzadeh-Rezaie, J. W. Cleary, "Electrodynamic properties of aqueous spray deposited SnO_2:F films for infrared plasmonics," Opt. Eng. 56, 037109 (2017).

[14] R. Gibson, S. Vangala, I. O. Oladeji, E. Smith, F. Khalizadeh-Rezaie, K. Leedy, R. E. Peale, and Justin W. Cleary, "Conformal spray-deposited fluorine-doped tin oxide for mid- and long-wave infrared plasmonics" Optical Materials Express 7, 2477 (2017).

[15] R. Soref, R. E. Peale, and W. Buchwald, "Longwave plasmonics on doped silicon and silicides," Optics Express 16, 6507 (2008).

[16] R. Peale, J. Cleary, D. Shelton, G. Boreman, R. Soref, W. Buchwald, "Silicides for Infrared Surface Plasmon Resonance Biosensors," Proc. Mat. Res. Soc. 1133-AA10-03 (2008).

[17] J. W. Cleary, R. E. Peale, D. J. Shelton, G. D. Boreman, C. W. Smith, M. Ishigami, R. Soref, A. Drehman, W.R. Buchwald, "IR permittivities for silicides and doped silicon," JOSA B 27, 730-734 (2010).

[18] J. W. Cleary, G. Medhi, M. Shahzad, I. Rezadad, D. Maukonen, R. E. Peale, G. D. Boreman, S. Wentzell, and W. R. Buchwald, "Infrared surface polaritons on antimony," Optics Express 20, 2693 (2012).

[19] J. W. Cleary, W. H. Streyer, N. Nader, S. Vangala, I. Avrutsky, B. Claflin, J. Hendrickson, D. Wasserman, R. E. Peale, W. Buchwald, and R. Soref, "Platinum germanides for mid- and long-wave infrared plasmonics," Optics Express 23, 3316 (2015).

[20] F. Khalilzadeh-Rezaie, C. W. Smith, J. Nath, N. Nader, M. Shahzad, J. W. Cleary, I. Avrutsky, and R. E. Peale, "Infrared surface polaritons on bismuth," J. Nanophotonics 9, 093792 (2015).

[21] A. Boltasseva and H. A. Atwater, "Low-Loss Plasmonic Metamaterials," Science 331, 290 (2011).